Baseline scenarios of heat-related ambulance transportations under climate change in Tokyo, Japan

Marie Fujimoto [1], **Hiroshi Nishiura** [Corresp. 1]

[1] School of Public Health, Kyoto University, Kyoto, Japan

Corresponding Author: Hiroshi Nishiura
Email address: nishiurah@gmail.com

Background. Predictive scenarios of heatstroke over the long-term future have yet to be formulated. The purpose of the present study was to generate baseline scenarios of heat-related ambulance transportations using climate change scenario datasets in Tokyo, Japan.

Methods. Data on the number of heat-related ambulance transportations in Tokyo from 2015 to 2019 were examined, and the relationship between the risk of heat-related ambulance transportations and the daily maximum wet-bulb globe temperature (WBGT) was modeled using three simple dose–response models. To quantify the risk of heatstroke, future climatological variables were then retrieved to compute the WBGT up to the year 2100 from climate change scenarios (i.e., RCP2.6, RCP4.5, and RCP8.5) using two scenario models. The predicted risk of heat-related ambulance transportations was embedded onto the future age-specific projected population.

Results. The proportion of the number of days with a WBGT above 28°C is predicted to increase every five years by 0.16% for RCP2.6, 0.31% for RCP4.5, and 0.68% for RCP8.5. In 2100, compared with 2000, the number of heat-related ambulance transportations is predicted to be more than three times greater among people aged 0–64 years and six times greater among people aged 65 years or older. The variance of the heatstroke risk becomes greater as the WBGT increases.

Conclusions. The increased risk of heatstroke for the long-term future was demonstrated using a simple statistical approach. Even with the RCP2.6 scenario, with the mildest impact of global warming, the risk of heatstroke is expected to increase. The future course of heatstroke predicted by our approach acts as a baseline for future studies.

1 **TITLE**

2 Baseline scenarios of heat-related ambulance transportations under climate change in Tokyo,

3 Japan

5 **Authors:**

6 Marie Fujimoto[1] and Hiroshi Nishiura[1]

8 **Affiliations:**

9 [1]Kyoto University School of Public Health, Yoshidakonoe cho, Sakyo-ku, Kyoto City 6068501,

10 Japan

12 Corresponding Author:

13 Hiroshi Nishiura[1]

14 Kyoto University School of Public Health

15 Yoshidakonoecho, Sakyo-ku, Kyoto 6068501, Japan

16 Tel: +81 75 753 4456, Fax: +81 75 753 4458

17 Email address: nishiura.hiroshi.5r@kyoto-u.ac.jp

18   **Abstract (500 words)**

19   **Background**. Predictive scenarios of heatstroke over the long-term future have yet to be

20   formulated. The purpose of the present study was to generate baseline scenarios of heat-related

21   ambulance transportations using climate change scenario datasets in Tokyo, Japan.

22   **Methods**. Data on the number of heat-related ambulance transportations in Tokyo from 2015 to

23   2019 were examined, and the relationship between the risk of heat-related ambulance

24   transportations and the daily maximum wet-bulb globe temperature (WBGT) was modeled using

25   three simple dose–response models. To quantify the risk of heatstroke, future climatological

26   variables were then retrieved to compute the WBGT up to the year 2100 from climate change

27   scenarios (i.e., RCP2.6, RCP4.5, and RCP8.5) using two scenario models. The predicted risk of

28   heat-related ambulance transportations was embedded onto the future age-specific projected

29   population.

30   **Results**. The proportion of the number of days with a WBGT above 28°C is predicted to

31   increase every five years by 0.16% for RCP2.6, 0.31% for RCP4.5, and 0.68% for RCP8.5. In

32   2100, compared with 2000, the number of heat-related ambulance transportations is predicted to

33   be more than three times greater among people aged 0–64 years and six times greater among

34   people aged 65 years or older. The variance of the heatstroke risk becomes greater as the WBGT

35   increases.

36   **Conclusions**. The increased risk of heatstroke for the long-term future was demonstrated using a

37   simple statistical approach. Even with the RCP2.6 scenario, with the mildest impact of global

38   warming, the risk of heatstroke is expected to increase. The future course of heatstroke predicted

39   by our approach acts as a baseline for future studies.

40   **Keywords**

41   Statistical model; global warming; heatstroke; adaptation; Forecasting; CMIP6

42   **Introduction**

43   Heatstroke is a heat-related illness in which a patient becomes unable to control his or her own

44   body temperature because of continuous exposure to a warm environment (Bouchama &

45   Knochel, 2022). In the United States, 7,000 patients were reported to have died of heatstroke

46   from 1979 to 1997 (Centers for Disease Control and Prevention, 2000). In France, over 15,000

47   excess deaths are estimated to have arisen from the 2003 heat wave (Vandentorren et al., 2006).

48   Another study in the United Kingdom documented 892 excess deaths in the summer that resulted

49   from three heatwaves in 2019 (Brimicombe et al., 2021), and called for a more inclusive

50   approach to heat waves including an intensified mitigation policy against climate change. In

51   Japan, heatstroke patients in the summer account for 1% of annual emergency transportations,

52   and more than half of these are aged 65 years or older (Fire and Disaster Management Agency,

53   2022a; Fire and Disaster Management Agency, 2022b). As a "super-aged" nation, the country

54   expects a continuing increase in the incidence of heatstroke, possibly with an exacerbation of

55   prognosis because of aging within the elderly population.

56   In the area of climate change, physical studies of risks associated with natural disasters,

57   including the highest temperature of the year (Papalexiou et al., 2018) and hydro-meteorological

58   hazards (Debele et al., 2019), have been extensively conducted, but there have been relatively

59   few studies of health-related outcomes. The small number of health-related studies include

60   predictive analyses of the health effects—particularly mortality, as well as heat stress disorder—

61   of uncomfortable temperatures; these have been conducted on a national scale (Barnett et al.,

62   2010; Fouillet et al., 2007; Kim et al., 2019; Lee, Röösli & Ragettli, 2021; Weinberger et al.,

63   2019), at a regional level (Dimitriadou et al., 2022; Scovronick et al., 2018), and on a global

64 scale (Guo et al., 2017; Mistry et al., 2022). Heat-related health events are usually observed

65 among elderly people, and therefore more effective countermeasures for protecting elderly

66 people are required (Rodrigues et al., 2020; Ragettli et al., 2017). Sheffield et al. (2018) showed

67 that health effects of heat waves depend on age and race (or ethnicity), and occur even among

68 children younger than five years old, who are considered as vulnerable as elderly people.

69 Predictive models of heatstroke have been studied with the eventual aim of preventing the

70 disease and reducing the associated mortality. The wet-bulb globe temperature (WBGT) is

71 known to be a useful environmental predictor of heatstroke events (Budd, 2008; Ueno et al.,

72 2021). The unit of WBGT is the same as that of temperature. WBGT is divided into five levels

73 to alert people to heatstroke, and action policies are provided for each level. The five levels are:

74 less than 21°C, 21°C to 25°C, 25°C to 28°C, 28°C to 31°C, and 31°C or more (Asayama, 2009).

75 In Japan, the Ministry of the Environment regularly communicates the risk of heatstroke, raising

76 public awareness to promote prevention, and WBGT thresholds 28°C and 31°C are used for

77 elevating the level of warning messages. When the WBGT exceeds 28°C, the risk of developing

78 heatstroke is said to increase, acting as a social trigger for the cancelation of events, for example,

79 the cessation of exercise (The American College of Sports Medicine, 2022; Japan Sports

80 Association, 2013). In Japan, an epidemiological study was conducted to predict the prevalence

81 of heatstroke among elderly patients in an indoor environment (Kodera et al., 2019). Moreover,

82 machine learning has been employed to attempt to better predict such events over the course of

83 time (Ogata et al., 2021; Ikeda & Kusaka, 2021). Nevertheless, predictive scenarios over the

84 long-term future have yet to be formulated. Because of the availability of climate change forecast

85 scenarios—such as those based on the Coupled Model Intercomparison Project Phase 6

86 (CMIP6)—climatological variables in high spatial and temporal resolutions are readily available

87 for the long-term future (e.g., up to the year 2100).

88 The purpose of the present study was to generate baseline scenarios of heat-related

89 ambulance transportations in Tokyo, Japan using climate change scenario datasets. We

90 specifically explored Tokyo, because Tokyo is the prefecture with the highest number of

91 heatstroke transportations per year. Severe heatstroke cases are predicted for the long-term future

92 using climatological data, particularly the WBGT because it is easily computed from

93 meteorological variables (Ono & Tonouchi, 2014). Whereas it is known that computing WBGT

94 is technically complicated, a simplified WBGT exists as an approximation, acting as a publicly-

95 used indicator of heat stress along with environmental stress index (Kong & Huber, 2022).

96 Baseline scenarios will be useful for understanding the possible future course of heatstroke,

97 thereby providing a basis on which interventions, particularly adaptation policies, can be

98 designed.

99 **Materials & Methods**

100 **Epidemiological data**

101 To construct a forecast model, we used heat-related ambulance transportation data for the

102 period from 2015 to 2019. The latest two years, 2020 and 2021, were omitted to disregard the

103 impact of coronavirus disease (COVID-19) on associated behaviors (e.g., a stay-home policy

104 was in place during the pandemic). Specifically, we used a dataset on the daily number of people

105 transported by ambulance for heatstroke, which records every single transportation event and is

106 openly published by the Fire and Disaster Management Agency (2022a). The ambulance

107 transportation case data were structured by age group; in the following analysis, we analyze the

108   data by dividing the population into three age groups: 0–17 years, 18–64 years, and 65 years or

109   older. In addition to case data, data on the daily maximum WBGT were obtained from the

110   Ministry of the Environment (2022). In addition, the population size for Tokyo for the period

111   from 2015 to 2019 in the abovementioned three age groups was obtained (Tokyo Metropolitan

112   Government, 2022) to calculate the risk of heat-related ambulance transportations. For instance,

113   in 2019, the population sizes of 0–17 years, 18–64 years, and 65 years or older were 1.86

114   million, 8.25 million and 3.08 million, respectively, and of these, 553, 2322 and 3171 heatstroke

115   cases called for ambulance transportation.

116   The Intergovernmental Panel on Climate Change (IPCC) released its AR6 on August 9,

117   2021. They found that, by at least the late 2030s, global average temperatures are likely to have

118   increased by 1.5°C above pre-industrial levels (IPCC, 2021). In the present study, we obtained

119   climate change scenarios based on CMIP6, published by the National Institute for Environmental

120   Studies (Ishizaki, 2021). Of the five different scenario models available, we selected two: (i)

121   Model for Interdisciplinary Research on Climate version 6 (MIROC6), which was cooperatively

122   developed by a Japanese modeling community to precisely reflect the meteorological conditions

123   in Japan, and (ii) Meteorological Research Institute Earth System Model version 2.0 (MRI-ESM-

124   2.0), which was developed by the Japan Meteorological Agency and offers accurate forecasts of

125   rainfall and humidity. MRI-ESM-2.0 was adopted because humidity plays a critical role in

126   calculating the WBGT. For each model, three different time-series scenarios—Representative

127   Concentration Pathway (RCP) 2.6, RCP4.5, and RCP8.5—with daily climatological data from

128   1900 to 2100 were obtained for each 1-km square of geographic mesh. Using the two models and

129   three time-series scenarios, the daily maximum temperature, relative humidity, total solar

130   radiation, and average wind speed in a geographic space that contains the Imperial Palace of

131   Japan, located in central Tokyo, were extracted to calculate the WBGT for each date (Ono &

132   Tonouchi, 2014). The reason why we chose the area around the Imperial Palace as the location of

133   our analysis is that data on the daily maximum WBGT were consistently available for this

134   particular geographic space over the whole time period.

135   **Mathematical model**

136   For the purpose of prediction, we exploited the relationship between the number of heat-

137   related ambulance transportations per million population and the daily maximum WBGT. These

138   heatstroke data were used to predict the per capita risk because we subsequently used the

139   estimate multiplied by the predicted age-specific population size during the forecasting process.

140   The model was fitted by age group (i.e., 0–17 years, 18–64 years, and 65 years or older). Several

141   different statistical models were employed to describe the dose–response relationship. The first is

142   a classical model that captures a monotonic increase in the risk of heatstroke as a linear function

143   of the WBGT after the WBGT exceeds a threshold value; this is referred to as the hockey stick

144   regression method (Yanagimoto & Yamamoto, 1979). This classical model was specifically

145   revisited because there is an existing notion of a threshold around a WBGT of 28°C. Using the

146   daily maximum WBGT (T), the number of heat-related ambulance transportations per million

147   population $n(T)$ was modeled as

$$E(n(\mathrm{T})) = \begin{cases} \beta_1 & , \text{for } T < T_w \\ \beta_1 + \beta_2(\mathrm{T} - T_w), & \text{for } T_w \leq T \end{cases} \tag{1}$$

148   where T_w is the WBGT threshold above which the risk of heatstroke abruptly increases. β_1 is the

149   constant risk at a WBGT below T_w; β_2 is the gradient of risk when the WGBT exceeds T_w. The

150   model was independently fitted to each age group, and T_w was treated as a parameter because

151 different age groups were expected to have different threshold levels (i.e., different physical

152 endurance levels).

153 The second model is an extension of the first. Frequently, the WBGT is expressed as one

154 of five discrete levels, with the highest level being a WBGT of 31°C or more; this implies

155 another threshold that boosts the risk of heatstroke. With two threshold temperatures, T_{w1} and

156 T_{w2}, the expected number of transportations per million population $n(T)$ was modeled as

$$E(n(T)) = \begin{cases} \beta_1 & , \quad \text{for } T < T_{w1} \\ \beta_1 + \beta_2(T - T_{w1}) & , \text{for } T_{w1} \leq T < T_{w2} \\ \beta_1 + \beta_2(T_{w2} - T_{w1}) + \beta_3(T - T_{w2}) & , \quad \text{for } T_{w2} \leq T \end{cases} \tag{2}$$

157 where β_1 is the constant risk at a WBGT below T_{w1} and β_2 and β_3 are the gradients of risk when

158 the WBGT exceeds 28°C and 31°C, respectively.

159 The third model is a phenomenological model that assumes an exponential increase in the

160 risk of heatstroke. We allowed a threshold for this model as well. Let r be the exponential rate of

161 increase in risk and let β_1 be the constant risk below the WBGT threshold. We have

$$E(n(T)) = \begin{cases} \beta_1 & , \text{for } T < T_w \\ \beta_1 exp(r(T - T_w)), & \text{for } T_w \leq T \end{cases} \tag{3}$$

162 Assuming that the variations in the observed counts of heat-related ambulance transportations are

163 sufficiently captured by a Poisson distribution with the expectation given by (1), (2), or (3),

164 maximum likelihood estimation was performed to obtain optimal values of the parameters. The

165 Akaike information criterion (AIC) was calculated to compare the model fit. The mean absolute

166 error (MAE) of the prediction from the observed values was also calculated to evaluate the

167 accuracy of prediction.

168 **Future prediction scenarios of heat-related ambulance transportations**

169 We consistently used the following formula to calculate the WBGT from readily

170 available climatological data (Ono & Tonouchi, 2014):

$$T_{WBGT} = 0.735 \times T_{asmax} + 0.0374 \times RH + 0.00292 \times T_{asmax} \times RH + 7.619 \times SR - 4.557 \times SR^2 \\ WS - 4.064 \quad (4)$$

171   which is most frequently used in Japan to estimate the WBGT. T_{asmax} is the maximum daily

172   temperature (°C), RH is the relative humidity (%) , SR is global solar radiation (kW/m²)

173   measured by horizontally installed solar radiation meter , and WS is the average wind speed

174   (m/s). A validation study of this approximate equation has excellently shown that 98.3% to

175   99.8% of WBGT estimate involved a bias less than 1.0°C. In Japan, WBGT is physically

176   measured in 11 different locations (weather observatories), and an approximate WBGT using

177   equation (4) has been officially adopted in other 829 observatory stations. The MIROC6 and

178   MRI-ESM-2.0 meteorological data were substituted into (4) to calculate the daily WBGT values

179   from 2000 to 2100. Because the bifurcation of temperature change begins in 2015 in the two

180   climate change models, data from 2000 to 2014 were calculated using common data.

181   In each future year, the proportion of days with a WBGT value falling into each of five

182   discrete ranges was calculated. This was calculated as the number of days with a WBGT value in

183   each range divided by the total number of days (365). Because climatological variables fluctuate

184   from year to year, the abovementioned proportions were calculated for every five years.

185   We examined the projected trends in the number of heat-related ambulance

186   transportations, explicitly accounting for future demography. To do so, we first calculated the

187   WBGT from May 1 to September 30 in each year, and used models (1), (2), and (3) to calculate

188   the risk per million population. Even in the long-term future, we assumed that the heatstroke risk

189   would occur only between May and September. The predicted risk was embedded onto the

190   projected age-specific populations aged 0–14 years, 15–64 years, and 65 years or older in the

191   period 2015–2100 (The Climate Change Adaptation Information Platform, 2022). To calculate

192   the 95% confidence intervals of our predictions of heat-related ambulance transportations, the

193   parametric bootstrapping method was employed, because parameters were inferred by maximum

194   likelihood method and the variance-covariance matrix was reasonably computed. To account for

195   parameter uncertainties of models (1), (2), and (3), 5,000 bootstrap resampling experiments were

196   conducted and the 2.5th and 97.5th percentile points were taken.

Data sharing statement

198   All datasets, including modeled climatological data for the period 2015–2100 and empirical data

199   on heat-related ambulance transportations for the period 2015–2019 in Tokyo are openly shared

200   as the online supporting material (Supplemental Tables S1, S2, S3 and S4).

Ethical considerations

202   The present study used publicly available information. Because no private information was used,

203   ethical approval was not required.

Results

205   Table 1 shows point estimates and 95% confidence intervals of the parameters for the

206   three models. The models differed in the WBGT threshold value above which the risk of

207   heatstroke begins to increase. It is worth noting that the estimated threshold temperature for

208   elderly people (those aged 65 years or older) was lower than that for the other age groups in all

209   three models. Of the three examined models, the exponential model yielded the smallest AIC for

210   all age groups, and thus was deemed the best-fit model.

211   Figure 1 shows a comparison between the observed and predicted data for heat-related

212   ambulance transportations, as predicted by using the WBGT. Both the dose–response

213   phenomena of heatstroke incidence depending on the WBGT and variations in the risk

214   depending on the WBGT should be noted. The observed data indicate that the risk of heatstroke

215   became increasingly variable as the WBGT increased. In particular, there was a large variation in

216   the risk of heatstroke in people aged 65 years or older, potentially reflecting the natural

217   adaptation behaviors that may have been adopted when the WGBT became extremely high.

218   Figure 2 shows the distribution of MAE as a function of WBGT, by age group. In

219   common with the abovementioned findings from Fig. 1, the MAE showed an increasing trend as

220   the WBGT increased, and this phenomenon was observed for all three models that we examined.

221   Using the hockey stick model, the maximum MAE was in people aged 65 years or older, with

222   the value 31.1. Similarly, the maximum MAE with the two-step hockey stick model was 28.6 in

223   the same age group. When the exponential model was employed, the maximum MAE was 28.1,

224   again in people aged 65 years or older.

225   Figure 3 shows the time-dependent change in the proportion of high WBGT values in the

226   long-term future, for each of the three climate change scenarios using two climate models (i.e.,

227   MIROC6 and MRI-ESM-2.0). Using MIROC6, the number of days with a WBGT above 28°C

228   increased every five years by 0.16% for RCP2.6, 0.31% for RCP4.5, and 0.68% for RCP8.5.

229   Similarly, using MRI-ESM-2.0, the number of days with a WBGT above 28°C increased every

230   five years by 0.20% for RCP2.6, 0.41% for RCP4.5, and 0.67% for RCP8.5. One noteworthy

231   point is that the proportion of days with a WBGT above 31°C monotonically increased in both

232   models for all climate change scenarios.

233   Figure 4 shows the long-term forecast of heat-related ambulance transportations for the

234   period 2000–2100 for each climate change scenario and model, using MIROC6. Even when the

235   hockey stick model was employed with the RCP2.6 scenario (the combination that yielded the

236   mildest impact of global warming), the total number of ambulance transportations is predicted to

237   increase. In 2100, the numbers of heatstroke patients transported in the groups aged 0–14 and

238   15–64 years are projected to be about three times higher than the numbers observed in 2000.

239   Among people aged 65 years or older, the number of ambulance transportations is expected to be

240   more than six times that observed in 2000. Figure 5 shows the same long-term forecast, based on

241   MRI-ESM-2.0. In general, the forecast is qualitatively identical to that derived from MIROC6.

242   The increase in risk over time among elderly people tends to be greater than that among younger

243   groups in both models.

244   **Discussion**

245   The present study developed a model to forecast heat-related ambulance transportations

246   for the long-term future until 2100 in Tokyo, Japan in various climate change scenarios and

247   using multiple climatological scenario models. In addition to the climatological scenarios and

248   models, three dose–response models were employed to predict the heat-related ambulance

249   transportations per million population as a function of the daily maximum WBGT, using

250   observations from 2015–19 as the training data. The elderly age group was revealed to have a

251   lower WBGT threshold than younger age groups. Our finding is consistent with published

252   studies which reported that the elderly age group tends to have a difficulty in regulating body

253   temperature under warm environmental conditions (Meade RD et al., 2020; Larose J et al.,

254   2013). Calculating the WBGT for RCP2.6, RCP4.5, and RCP8.5 for the scenario models, we

255   have shown that the proportion of days with a WBGT between 28°C and 31°C and the

256   proportion with a WGBT above 31°C will monotonically increase. Embedding the predicted risk

257   of heat-related ambulance transportations onto the future age-specific projected population, we

258   were able to objectively predict the increased risk of heatstroke for the long-term future using a

259 simple statistical approach. Even with the RCP2.6 scenario, which shows the mildest impact of

260 global warming, the risk of heatstroke was predicted to increase.

261 To the best of our knowledge, the present study is the first to predict the risk of heatstroke

262 using the proposed statistical dose-response modelling approach. The forecasting principles are

263 simple and tractable (e.g., using a dose–response model and embedding the risk onto the

264 projected population), and yet the model captures the essential mechanisms of the elevated risk

265 of heatstroke as a function of time. Only by quantifying the future risk of heatstroke, as practiced

266 in the present study, can we understand the quantitative magnitude of the future increase. The

267 future course of heatstroke predicted by our approach acts as a baseline for future studies. That

268 is, various adaptation policies (e.g., simply canceling outdoor events when the WBGT is

269 extreme) will be planned according to the baseline risks, and we will examine how far the risk of

270 heatstroke could be reduced by the adaptation efforts of society.

271 Of the three forecasting models that we examined, the exponential model yielded the

272 smallest AIC value, indicating that the dose–response relationship between the risk of heatstroke

273 and the WBGT is most appropriately captured by this model for all three age groups. This

274 finding indicates that the elevation of the risk of heatstroke is accelerated as the WBGT

275 increases. In the context of climate change, given that the higher the WBGT, the larger the error,

276 it is statistically challenging to successfully quantify the risk of heatstroke with an extremely

277 elevated WBGT in the future. The exponential model implies that the intrinsic risk of heatstroke

278 with a very high WBGT is likely to be far greater than what we explored in this study using

279 empirical data.

280 An important observation from the dose–response phenomena is that the variance of the

281 risk increased as the WBGT increased. In fact, using the simple dose–response models, the MAE

282   appeared to be large with high WBGT values. This variation was particularly noticeable among

283   people aged 65 years or older. We believe that this variation was caused partly by natural

284   adaptation behaviors. Because a high WBGT did not necessarily lead to large numbers of

285   ambulance transportations of heatstroke patients, it is possible that dynamic changes in the

286   WBGT may predict the risk of heatstroke better than the daily maximum WBGT. It has been

287   speculated that the incidence of heatstroke is increased by an inability to take adaptation

288   behaviors in each specific individual , such as participating in sports event or festivals among

289   young individuals (Kasai et al., 2017) and continuously laying down in a warm room among

290   elderly (Abrahamson et al., 2009). Also, the risk of heatstroke may be high when the WBGT

291   suddenly increases. However, if a heat wave includes several consecutive days with high WBGT

292   values, people may change their behavior to reduce the risk of heatstroke in the subsequent days.

293   To capture the observed risk more accurately using available climatological variables is a subject

294   for our future study.

295   As mentioned in Introduction, published studies using machine learning methods for

296   heatstroke prediction modelling have already been widely recognized (Ogata et al., 2021; Ikeda

297   & Kusaka, 2021). The aim of the present study was to generate a longer-term baseline scenario

298   for heatstroke emergency transportation in Tokyo, using a dataset of climate change scenarios

299   and possibly employing a more simplistic and yet tractable approach. To accomplish the goal, a

300   statistical dose-response modelling approach based on an approximate WBGT value was shown

301   to reasonably predict the number of heatstroke cases in future Japan.

302   There are three limitations that need to be discussed. First, the present study examined

303   only empirical data from Tokyo; thus, it is unclear whether its findings are applicable to a wider

304   geographic area of Japan. Forecasting must be extended to geographic regions other than Tokyo.

305   Second, the present study relied on ambulance transportation data, which represent only a small

306   fraction of heatstroke cases. Therefore, patients with mild heatstroke were not counted. However,

307   we believe that the overall time trends were captured even though only severe cases of heatstroke

308   were counted. Third, we must revisit the reliability of the forecasting model in the future. Wide

309   variations in the numbers of heat-related ambulance transportations when the WBGT value is

310   high imply that our model cannot capture the peaks and troughs of heatstroke incidence during

311   summer days with high WBGT values, particularly among people aged 65 years or older. There

312   is scope for improvement in the accuracy of the models.

313   Although several key tasks remain, we believe that the present study successfully

314   provided a baseline scenario for heatstroke in Tokyo for the future, until the year 2100, using a

315   simple statistical modeling approach. Various adaptation policies will be planned according to

316   the baseline risks, and we will examine how far the risk of heatstroke could be reduced by the

317   adaptation efforts of society.

318   **Conclusions**

319   In conclusion, we have shown that a simple dose-response model with WBGT as a

320   predictor can reasonably quantify the future increase in the number of heat stroke cases. The

321   present study developed a model to forecast heat-related ambulance transportations for the long-

322   term future, until 2100 in Tokyo, Japan in various climate change scenarios and using multiple

323   climatological scenario models. By calculating the WBGT for RCP2.6, RCP4.5, and RCP8.5 for

324   the scenario models, we have shown that the proportion of days with a WBGT between 28°C and

325   31°C and the proportion with a WGBT above 31°C will monotonically increase. Embedding the

326   predicted risk of heat-related ambulance transportations onto the future age-specific projected

327   population, we were able to objectively predict the increased risk of heatstroke for the long-term

328 future using a simple statistical approach. Even with the RCP2.6 scenario, which shows the

329 mildest impact of global warming, the risk of heatstroke was predicted to increase. The future

330 course of heatstroke predicted by our approach acts as a baseline for future studies.

331

332

333 **Funding**

334 This study was supported mainly by the Environment Research and Technology Development

335 Fund (JPMEERF20S11804) of the Environmental Restoration and Conservation Agency of

336 Japan. HN received funding from Health and Labor Sciences Research Grants (20CA2024,

337 20HA2007, 21HB1002 and 21HA2016), the Japan Agency for Medical Research and

338 Development (JP20fk0108140, JP20fk0108535, and JP21fk0108612), the JSPS KAKENHI

339 (21H03198), and the Japan Science and Technology Agency SICORP program (JPMJSC20U3

340 and JPMJSC2105). The funders had no role in the study design, data collection and analysis,

341 decision to publish, or preparation of the manuscript.

342 **Acknowledgments**

343 We thank Edanz Group (https://en-author-services.edanz.com/ac) for editing a draft of this

344 manuscript.

345 **Conflict of interest**

346 We declare that we have no conflict of interest.

347 **Data sharing statement**

348 All datasets, including modeled climatological data for the period 2015–2100 and empirical data

349 on heat-related ambulance transportations for the period 2015–2019 in Tokyo are openly shared

350 as the online supporting material (Supplemental Tables S1, S2, S3, and S4).

351 **Ethical considerations**

352 The present study used publicly available information. Because no private information was used,

353 ethical approval was not required.

354

355

356 **References**

357 Abrahamson V, Wolf J, Lorenzoni I, Fenn B, Kovats S, Wilkinson P, Adger WN, Raine R. 2009.

358 Perceptions of heatwave risks to health: interview-based study of older people in London and

359 Norwich, UK. *Journal of Public Health (Oxf)*. Mar;31(1):119-26.

360 Asayama, M. 2009. Guideline for the prevention of heat disorder in Japan. *Global environmental*

361 *research* 13:19-25.

362 Barnett AG, Tong S, Clements AC. 2010. What measure of temperature is the best predictor of

363 mortality? *Environmental Research* 110:604-611.

364 Bouchama A, Knochel JP. 2002. Heatstroke. *The New England Journal of Medicine* 346:1978-

365 1988.

366 Brimicombe C, Porter JJ, Di Napoli C, Pappenberger F, Cornforth R, Petty C, Cloke HL. 2021.

367 Heatwaves: An invisible risk in UK policy and research. *Environmental Science & Policy* 116:1-

368 7.

369 Budd GM. 2008. Wet-bulb globe temperature (WBGT)—its history and its limitations. *Journal*

370 *of Science and Medicine in Sport* 11:20-32.

371   Centers for Disease Control and Prevention (CDC). 2000. Heat-related illnesses, deaths, and risk

372   factors—Cincinnati and Dayton, Ohio, 1999, and United States, 1979–1997. *Morbidity and*

373   *Mortality Weekly Report* 49:470-473.

374   Debele SE, Kumar P, Sahani J, Marti-Cardona B, Mickovski SB, Leo LS, Porcù F, Bertini F,

375   Montesi D, Vojinovic Z, Di Sabatino S. 2019. Nature-based solutions for hydro-meteorological

376   hazards: Revised concepts, classification schemes and databases. *Environmental Research*

377   179(Part B):108799.

378   Dimitriadou L, Nastos P, Eleftheratos K, Kapsomenakis J, Zerefos C. 2022. Mortality related to

379   air temperature in European cities, based on threshold regression models. *International Journal*

380   *of Environmental Research and Public Health* 19:4017.

381   Fouillet A, Rey G, Jougla E, Frayssinet P, Bessemoulin P, Hémon D. 2007. A predictive model

382   relating daily fluctuations in summer temperatures and mortality rates. *BMC Public Health*

383   7:114.

384   Fire and Disaster Management Agency (FDMA). 2022a. Current status of emergency rescue.

385   Available at https://www.fdma.go.jp/publication/#rescue (accessed 20 April 2022)

386   Fire and Disaster Management Agency (FDMA). 2022b. Data on emergency transport personnel

387   due to heatstroke. Available at https://www.fdma.go.jp/disaster/heatstroke/post3.html (accessed

388   20 April 2022)

389   Guo Y, Gasparrini A, Armstrong BG, Tawatsupa B, Tobias A, Lavigne E, Coelho MSZS, Pan X,

390   Kim H, Hashizume M, Honda Y, Guo YL, Wu CF, Zanobetti A, Schwartz JD, Bell ML,

391   Scortichini M, Michelozzi P, Punnasiri K, Li S, Tian L, Garcia SDO, Seposo X, Overcenco A,

392   Zeka A, Goodman P, Dang TN, Dung DV, Mayvaneh F, Saldiva PHN, Williams G, Tong S.

393   2017. Heat wave and mortality: A multicountry, multicommunity study. *Environmental Health*

394   *Perspectives*125:087006.

395   Ikeda T, Kusaka H. 2021. Development of models for predicting the number of patients with

396   heatstroke on the next day considering heat acclimatization. *Journal of the Meteorological*

397   *Society of Japan.* 99:1395-1412.

398   Ishizaki N. 2021. Bias corrected climate scenarios over Japan based on CDFDM method using

399   CMIP6, Ver.1. National Institute for Environmental Studies (NIES). DOI:

400   10.17595/20210501.001 (accessed 23 December 2021)

401   Japan Sports Association (JSPO). 2013. Exercise guidelines for heatstroke prevention. Available

402   at https://www.japan-sports.or.jp/medicine/heatstroke/tabid922.html (in Japanese) (accessed 20

403   April 2022)

404   Kasai M, Okaze T, Mochida A, Hanaoka K. 2017. Heatstroke Risk Predictions for Current and

405   Near-Future Summers in Sendai, Japan, Based on Mesoscale WRF Simulations. *Sustainability.*

406   2017; 9(8):1467

407   Kim DW, Deo RC, Park SJ, Lee JS, Lee WS. 2019. Weekly heat wave death prediction model

408   using zero-inflated regression approach. *Theoretical and Applied Climatology* 137:823-838.

409   Kodera S, Nishimura T, Rashed EA, Hasegawa K, Takeuchi I, Egawa R, Hirata A. 2019.

410   Estimation of heat-related morbidity from weather data: A computational study in three

411   prefectures of Japan over 2013–2018. *Environment International* 130:104907.

412   Kong Q, Huber M. 2022. Explicit calculations of wet-bulb globe temperature compared with

413   approximations and why it matters for labor productivity. *Earth's Future* 10, e2021EF002334.

414   Larose J, Wright HE, Stapleton J, Sigal RJ, Boulay P, Hardcastle S, Kenny GP. 2013. Whole

415   body heat loss is reduced in older males during short bouts of intermittent exercise. *American*

416 *Journal of Physiology - Regulatory Integrative and Comparative Physiology* Sep

417 15;305(6):R619-29.

418 Lee JY, Röösli M, Ragettli MS. 2021. Estimation of heat-attributable mortality using the cross-

419 validated best temperature metric in Switzerland and South Korea. *International Journal of*

420 *Environmental Research and Public Health* 18:6413.

421 Meade RD, Akerman AP, Notley SR, McGinn R, Poirier P, Gosselin P, Kenny GP. 2020.

422 Physiological factors characterizing heat-vulnerable older adults: A narrative review. *Environ*

423 *Internstional* Nov; 144:105909.

424 Mistry MN, Schneider R, Masselot P, Royé D, Armstrong B, Kyselý J, Orru H, Sera F, Tong S,

425 Lavigne É, Urban A, Madureira J, García-León D, Ibarreta D, Ciscar JC, Feyen L, de Schrijver

426 E, de Sousa Zanotti Stagliorio Coelho M, Pascal M, Tobias A, Multi-Country Multi-City (MCC)

427 Collaborative Research Network, Guo Y, Vicedo-Cabrera AM, Gasparrini A. 2022. Comparison

428 of weather station and climate reanalysis data for modelling temperature-related mortality.

429 *Scientific Reports* 12:5178.

430 Ogata S, Takegami M, Ozaki T, Nakashima T, Onozuka D, Murata S, Nakaoku Y, Suzuki K,

431 Hagihara A, Noguchi T, Iihara K, Kitazume K, Morioka T, Yamazaki S, Yoshida T, Yamagata

432 Y, Nishimura K. 2021. Heatstroke predictions by machine learning, weather information, and an

433 all-population registry for 12-hour heatstroke alerts. *Nature Communications* 12:4575.

434 Ono M, Tonouchi M. 2014. Estimation of wet-bulb globe temperature using generally measured

435 meteorological indices. *JAPANESE JOURNAL OF BIOMETEOROLOGY* 50:147-157.

436 Papalexiou SM, AghaKouchak A, Trenberth KE, Foufoula-Georgiou E. 2018. Global, regional,

437 and megacity trends in the highest temperature of the year: Diagnostics and evidence for

438 accelerating trends. *Earth's Future* 6:71-79.

439 Ragettli MS, Vicedo-Cabrera AM, Schindler C, Röösli M. 2017. Exploring the association

440 between heat and mortality in Switzerland between 1995 and 2013. *Environmental Research*

441 158:703-709.

442 Rodrigues M, Santana P, Rocha A. 2020. Statistical modelling of temperature-attributable deaths

443 in Portuguese metropolitan areas under climate change: Who is at risk? *Atmosphere* 11:159.

444 Scovronick N, Sera F, Acquaotta F, Garzena D, Fratianni S, Wright CY, Gasparrini A. 2018. The

445 association between ambient temperature and mortality in South Africa: A time-series analysis.

446 *Environmental Research* 161:229-235.

447 Sheffield PE, Herrera MT, Kinnee EJ, Clougherty JE. 2018. Not so little differences: variation in

448 hot weather risk to young children in New York City. *Public Health* 161:119-126.

449 The American College of Sports Medicine (ACSM). 2022. Heat and humidity guidelines for

450 races. Available at https://www.rrm.com/Newsarchives/archive11/11heat.htm (accessed 20 April

451 2022)

452 The Climate Change Adaptation Information Platform. 2022. Results of Environmental Research

453 Promotion Fund 2-1805 (Japanese SSP Population Scenarios by Municipality, Version 2).

454 Available at https://adaptation-platform.nies.go.jp/socioeconomic/population.html (accessed 20

455 April 2022)

456 The Ministry of the Environment, Government of Japan (MOE). 2022. Heat illness prevention

457 information. Available at https://www.wbgt.env.go.jp/wbgt_data.php (accessed 20 April 2022)

458 The Intergovernmental Panel on Climate Change (IPCC). 2021. AR6 Climate change 2021: The

459 physical science basis. Available at https://www.ipcc.ch/report/sixth-assessment-report-working-

460 group-i/ (accessed 20 April 2022)

461   Tokyo Metropolitan Government (TMG). 2022. Households and population in Tokyo based on

462   the basic resident register. Available at https://www.toukei.metro.tokyo.lg.jp/juukiy/jy-index.htm

463   (accessed 20 April 2022)

464   Ueno S, Hayano D, Noguchi E, Aruga T. 2021. Investigating age and regional effects on the

465   relation between the incidence of heat-related ambulance transport and daily maximum

466   temperature or WBGT. *Environmental Health and Preventive Medicine* 26:116.

467   Vandentorren S, Bretin P, Zeghnoun A, Mandereau-Bruno L, Croisier A, Cochet C, Ribéron J,

468   Siberan I, Declercq B, Ledrans M. 2006. August 2003 heat wave in France: risk factors for death

469   of elderly people living at home. *European Journal of Public Health* 16:583-591.

470   Weinberger KR, Spangler KR, Zanobetti A, Schwartz JD, Wellenius GA. 2019. Comparison of

471   temperature–mortality associations estimated with different exposure metrics. *Environmental*

472   *epidemiology* 3:e072.

473   Yanagimoto T, Yamamoto E. 1979. Estimation of safe doses: critical review of the hockey stick

474   regression method. *Environmental Health Perspectives* 32:193-199.

475

476 **Table1: Parameter estimates and model fit of dose-response model for heat-related ambulance transport as a function of WBGT in Tokyo, 2015-**
477 **19**

Age	The hockey stick model				Two-step hockey stick model						Exponential model			
	AIC	T_w	β_1	β_2	AIC	T_{w1}	T_{w2}	β_1	β_2	β_3	AIC	T_w	r	β_1
0-17 years	2493.8	28.8	0.6	1.8	2467.3	28.0	30.8	0.6	0.8	3.0	2456.0	25.7	0.4	0.5
95%CI		(28.6-29.0)	(0.55-0.67)	(1.62-1.97)		(27.6-28.4)	(30.4-31.1)	(0.53-0.64)	(0.58-1.04)	(2.40-3.54)		(25.1-26.3)	(0.37-0.45)	(0.38-0.54)
18-64 years	1747.0	28.4	0.3	1.6	1650.8	26.1	30.6	0.2	0.5	3.1	1630.3	23.7	0.5	0.1
95%CI		(28.2-28.5)	(0.26-0.34)	(1.49-1.76)		(25.7-26.5)	(30.3-30.9)	(0.16-0.24)	(0.36-0.56)	(2.63-3.62)		(22.8-24.6)	(0.44-0.48)	(0.09-0.17)
65 years and older	3999.9	27.9	1.0	4.4	3671.2	25.5	30.5	0.6	1.4	9.0	3620.2	22.7	0.4	0.4
95%CI		(27.8-28.0)	(0.88-1.04)	(4.23-4.62)	☐	(25.3-25.7)	(30.3-30.7)	(0.52-0.67)	(1.22-1.50)	(8.16-9.79)	☐	(22.1-23.3)	(0.42-0.44)	(0.28-0.44)

478 Each model was fitted independently to the data by age group. We used heat-related ambulance transported data from 2015 -19 retrieved from the Fire and
479 Disaster Management Agency share. T_w represents threshold WBGT and its unit is Celsius degree. AIC stands for the Akaike Information Criterion,
480 calculated assuming it follows a Poisson distribution. The hockey stick model assumes that the risk of developing heatstroke increases linearly when the
481 WBGT exceeds the threshold T_w. Two-step hockey stick model assumes that the risk of developing heatstroke increases in a two-step manner, and the
482 boundary thresholds are T_{w1} and T_{w2}. The exponential formula assumes that the risk of developing heatstroke increases non-linearly when the WBGT
483 exceeds the threshold T_w. CI stands for the confidence interval as calculated from bootstrapping method.
484

485

486 **Figure legends**

487 **Figure 1: The risk of heat-related ambulance transportations as a function of wet-bulb**

488 **globe temperature (WBGT): a comparison between observed and predicted data.**

489 The vertical axis is the number of cases per million population per day, and the horizontal axis is

490 the daily maximum WBGT. The left, middle, and right panels show the age groups 0–17 years,

491 18–64 years, and 65 years or older, respectively. White circles represent observed values, solid

492 lines show the exponential model, long dashed lines show the two-step hockey stick model, and

493 dotted lines show the one-step hockey stick model.

494

495 **Figure 2: Mean absolute error between observed and predicted values, by age group.**

496 The mean absolute error (MAE) between the observed and predicted data is shown for each

497 model. Dots, white triangles, and crosses represent the MAE values for the age groups 0–17

498 years, 18–64 years, and 65 years or older, respectively. The MAE was calculated by dividing the

499 absolute difference between the observed and predicted values by the number of data points for

500 each identical wet-bulb globe temperature (WBGT) value.

501

502 **Figure 3: Future wet-bulb globe temperature (WBGT) patterns in Tokyo for the period**

503 **2000–2100.**

504 WBGT is represented as five discrete groups. The top two groups (i.e., a WBGT of 28–31°C and

505 a WGBT above 31°C) are regarded as having a particularly high risk of causing heatstroke. The

506 proportion of days that have each range of WBGT values was calculated for every period of five

507   years. The top and bottom panels show the projections for the MIROC6 scenario and the MRI-

508   ESM-2.0 scenario, respectively. The left, middle, and right columns show the predictions for the

509   RCP2.6, RCP4.5, and RCP8.5 temperature increase scenarios, respectively.

510

511   **Figure 4: Predicted number of heatstroke cases in Tokyo for the period 2000–2100, using**

512   **the MIROC6 scenario.**

513   The epidemiological prediction of the number of heat-related ambulance transportations for

514   every period of five years is shown, using the daily maximum wet-bulb globe temperature

515   (WBGT) derived from MIROC6. Predictions were made using the three statistical dose–response

516   models. The 95% confidence intervals were calculated using the parametric bootstrapping

517   method, and are represented by the shaded areas. The dotted and dashed line shows predictions

518   with RCP2.6, the dotted line shows predictions with RCP4.5, and the solid line shows

519   predictions with RCP8.5. The white circles represent observed data on heat-related ambulance

520   transportations for the five-year period beginning in 2015.

521

522   **Figure 5: Predicted number of heatstroke cases in Tokyo for the period 2000–2100, using**

523   **the MRI-ESM-2.0 scenario.**

524   The epidemiological prediction of the number of heat-related ambulance transportations for

525   every period of five years is shown, using the daily maximum wet-bulb globe temperature

526   (WBGT) derived from MRI-ESM-2.0. Predictions were made using the three statistical dose–

527   response models. The 95% confidence intervals were calculated using the parametric

528   bootstrapping method, and are represented by the shaded areas. The dotted and dashed line

529   shows predictions with RCP2.6, the dotted line shows predictions with RCP4.5, and the solid

530   line shows predictions with RCP8.5. The white circles represent observed data on heat-related

531   ambulance transportations for the five-year period beginning in 2015.

532

Figure 1

Figure 1: The risk of heat-related ambulance transportations as a function of wet-bulb globe temperature (WBGT): a comparison between observed and predicted data.

The vertical axis is the number of cases per million population per day, and the horizontal axis is the daily maximum WBGT. The left, middle, and right panels show the age groups 0–17 years, 18–64 years, and 65 years or older, respectively. White circles represent observed values, solid lines show the exponential model, long dashed lines show the two-step hockey stick model, and dotted lines show the one-step hockey stick model.
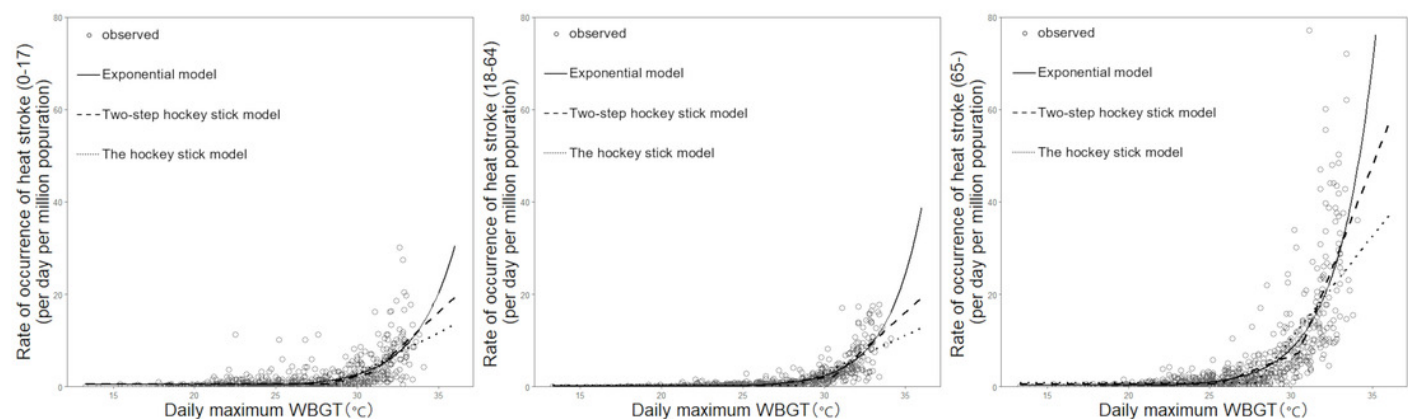
Figure 2

Figure 2: Mean absolute error between observed and predicted values, by age group.

The mean absolute error (MAE) between the observed and predicted data is shown for each model. Dots, white triangles, and crosses represent the MAE values for the age groups 0–17 years, 18–64 years, and 65 years or older, respectively. The MAE was calculated by dividing the absolute difference between the observed and predicted values by the number of data points for each identical wet-bulb globe temperature (WBGT) value.
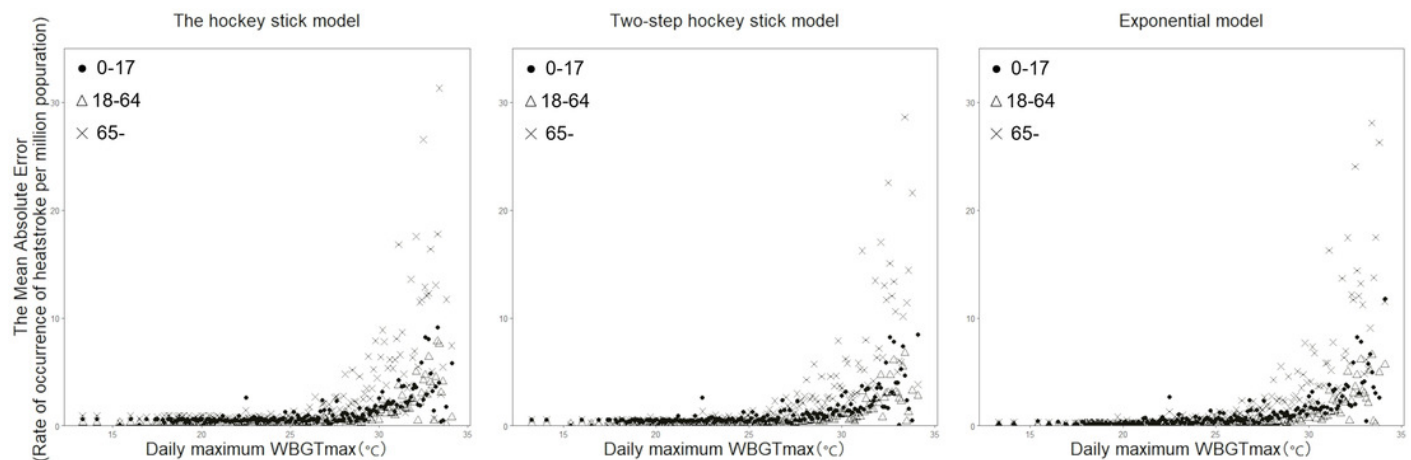
Figure 3

Figure 3: Future wet-bulb globe temperature (WBGT) patterns in Tokyo for the period 2000–2100.

WBGT is represented as five discrete groups. The top two groups (i.e., a WBGT of 28–31°C and a WGBT above 31°C) are regarded as having a particularly high risk of causing heatstroke. The proportion of days that have each range of WBGT values was calculated for every period of five years. The top and bottom panels show the projections for the MIROC6 scenario and the MRI-ESM-2.0 scenario, respectively. The left, middle, and right columns show the predictions for the RCP2.6, RCP4.5, and RCP8.5 temperature increase scenarios, respectively.
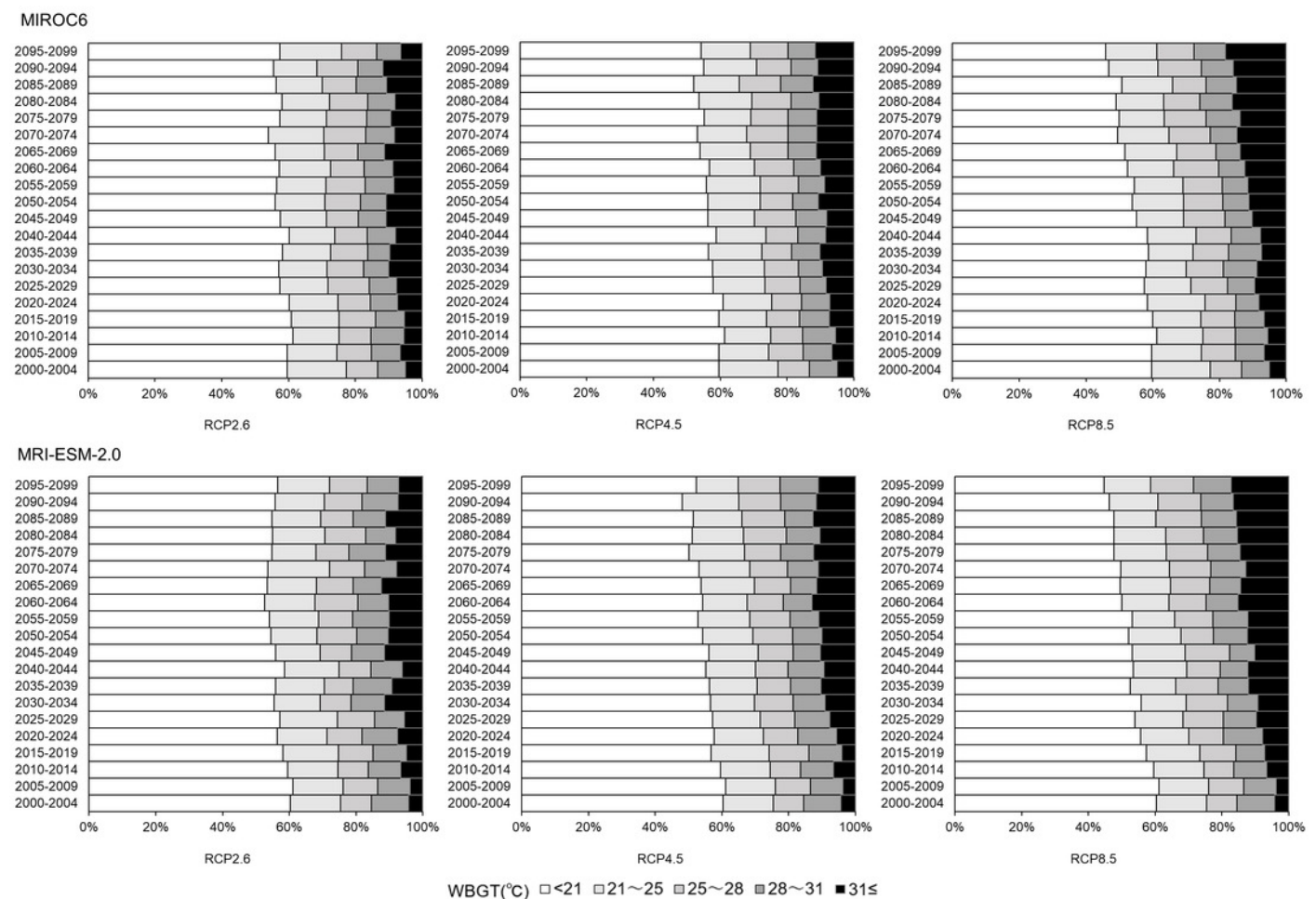
Figure 4

Figure 4: Predicted number of heatstroke cases in Tokyo for the period 2000–2100, using the MIROC6 scenario.

The epidemiological prediction of the number of heat-related ambulance transportations for every period of five years is shown, using the daily maximum wet-bulb globe temperature (WBGT) derived from MIROC6. Predictions were made using the three statistical dose–response models. The 95% confidence intervals were calculated using the parametric bootstrapping method, and are represented by the shaded areas. The dotted and dashed line shows predictions with RCP2.6, the dotted line shows predictions with RCP4.5, and the solid line shows predictions with RCP8.5. The white circles represent observed data on heat-related ambulance transportations for the five-year period beginning in 2015.

Predicted number of heatstroke cases in MIROC6
(from 0 to 14 y.o.)

The hockey stick model   Two-step hockey stick model   Exponential model

(from 15 to 64 y.o.)

The hockey stick model   Two-step hockey stick model   Exponential model

(over 65 y.o.)

The hockey stick model   Two-step hockey stick model   Exponential model
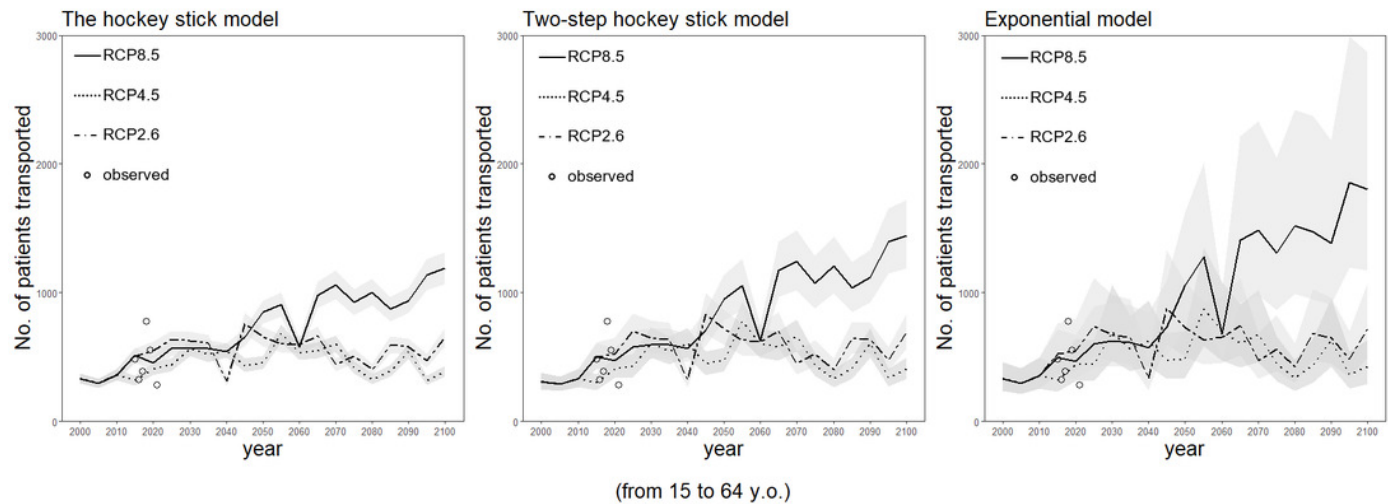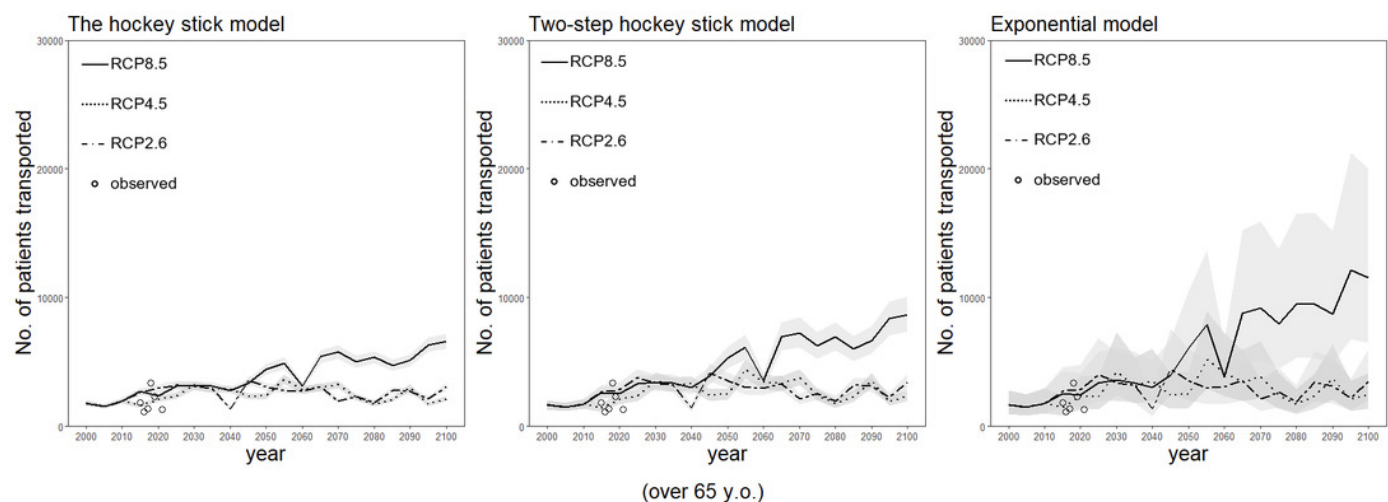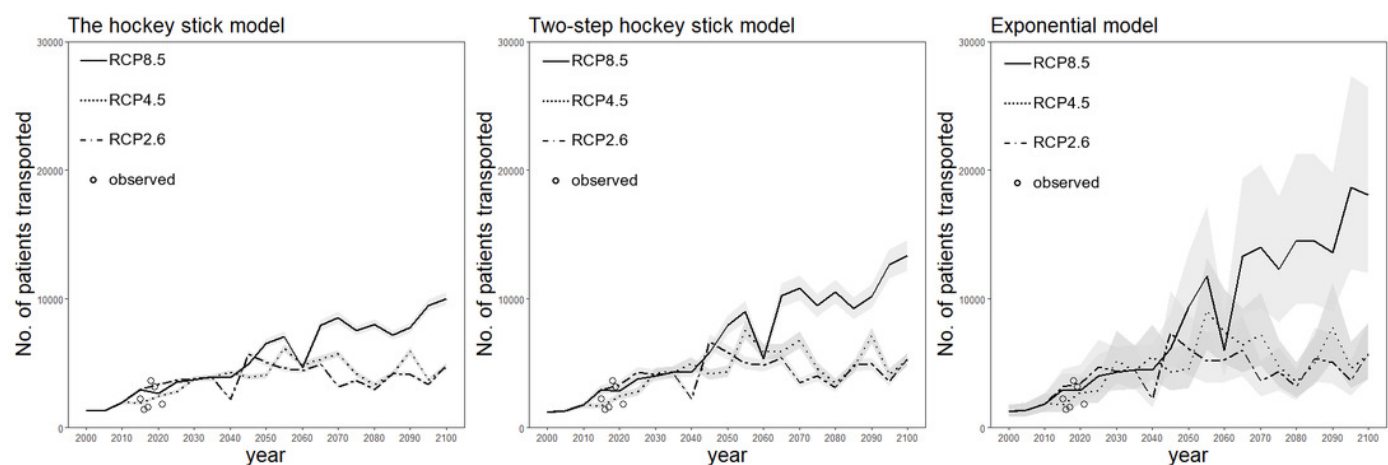
Figure 5

Figure 5: Predicted number of heatstroke cases in Tokyo for the period 2000–2100, using the MRI-ESM-2.0 scenario.

The epidemiological prediction of the number of heat-related ambulance transportations for every period of five years is shown, using the daily maximum wet-bulb globe temperature (WBGT) derived from MRI-ESM-2.0. Predictions were made using the three statistical dose–response models. The 95% confidence intervals were calculated using the parametric bootstrapping method, and are represented by the shaded areas. The dotted and dashed line shows predictions with RCP2.6, the dotted line shows predictions with RCP4.5, and the solid line shows predictions with RCP8.5. The white circles represent observed data on heat-related ambulance transportations for the five-year period beginning in 2015.

Predicted number of heatstroke cases in MRI-ESM-2.0
(from 0 to 14 y.o.)

The hockey stick model   Two-step hockey stick model   Exponential model

(from 15 to 64 y.o.)

The hockey stick model   Two-step hockey stick model   Exponential model

(over 65 y.o.)

The hockey stick model   Two-step hockey stick model   Exponential model